THE UNIVERSITY of EDINBURGH

Edinburgh Research Explorer

Identification of candidate host cell factors required for actin-based motility of Burkholderia pseudomallei

OPEN ACCESS

Article

Identification of candidate host cell factors required for actin-based motility of Burkholderia pseudomallei

Niramol Jitprasutwit, Nurhamimah Zainal-Abidin, Charles Vander Broek,
Dominic Kurian, Sunee Korbsrisate, Mark P Stevens, and Joanne M. Stevens

Just Accepted

Identification of candidate host cell factors required for actin-based motility of _Burkholderia pseudomallei_

Niramol Jitprasutwit[1&2], Nurhamimah Zainal-Abidin[1], Charles Vander Broek[1], Dominic Kurian[1], Sunee Korbsrisate[2], Mark P. Stevens[1] and Joanne M. Stevens[1*]

[1] The Roslin Institute and Royal (Dick) School of Veterinary Studies, University of Edinburgh, Easter Bush, Midlothian, EH25 9RG, United Kingdom.

[2] Department of Immunology, Faculty of Medicine Siriraj Hospital, Mahidol University Bangkok, Thailand.

[*]**Corresponding author**. The Roslin Institute and Royal (Dick) School of Veterinary Studies, University of Edinburgh, Easter Bush, Midlothian, EH25 9RG, United Kingdom. Tel. +44 131 651 9100. Fax. +44 131 651 9105. E-mail jo.stevens@roslin.ed.ac.uk

1

Abstract

Intracellular actin-based motility of the melioidosis pathogen *Burkholderia pseudomallei* requires the bacterial factor BimA. Located at one pole of the bacterium, BimA recruits and polymerises cellular actin to promote bacterial motility within and between cells. Here we describe an affinity approach coupled with Mass Spectrometry to identify cellular proteins recruited to BimA-expressing bacteria under conditions that promote actin polymerisation. We identified a group of cellular proteins that are recruited to the *B. pseudomallei* surface in a BimA-dependent manner, a subset of which were independently validated with specific antisera including the ubiquitous scaffold protein Ras GTPase-activating-like protein (IQGAP1). IQGAP1 integrates several key cellular signalling pathways including those involved in actin dynamics and has been shown to be involved in the adhesion of attaching and effacing *Escherichia coli* to infected cells and invasion of host cells by *Salmonella enterica* serovar Typhimurium. Whilst a direct interaction between BimA and IQGAP1 could not be detected using either conventional pulldown or yeast two hybrid techniques, confocal microscopy revealed that IQGAP1 is recruited to *B. pseudomallei* actin tails in infected cells and siRNA-mediated knockdown highlighted a role for this protein in controlling the length and actin density of *B. pseudomallei* actin tails.

2

Introduction

 Burkholderia pseudomallei causes melioidosis, a severe invasive infection of humans and animals endemic in Southeast Asia and Northern Australia. Human infections are acquired by inhalation, ingestion or via abraded skin and may produce a spectrum of disease ranging from rapidly fatal septicaemia and acute pneumonia, through chronic or localised abscess formation to subacute infections (reviewed in Wiersinga *et al.*[1]). Relapse and latency are common in melioidosis and it is believed that this reflects the ability of *B. pseudomallei* to persist in an intracellular niche and its intrinsic resistance to many classes of antibiotic.

 Facultative intracellular pathogens of several bacterial genera have evolved mechanisms to enter and exit eukaryotic cells by harnessing the power of actin polymerisation. Some species of *Burkholderia, Listeria*, *Mycobacterium*, *Rickettsia* and *Shigella* are propelled in the cytosol and into adjacent cells by polar nucleation of actin, a process termed actin-based motility. These bacteria use distinct mechanisms for actin-based motility, converging on activation of the cellular Arp2/3 complex by mimicry or recruitment of its regulators (reviewed in Stevens *et al.*[2]) or by mimicking Arp2/3-independent actin nucleators such as cellular formins or WH2–domain-containing proteins (reviewed in Qualmann and Kessels[3]). In the case of *Burkholderia* we discovered that this process requires BimA[4], a putative Type V secreted protein that is conserved amongst *B. pseudomallei* isolates in the endemic area[5]. *B. pseudomallei* BimA influences intracellular survival, intercellular spread[6] and virulence in mice[7], however the mechanism by which it recruits and activates cellular factors to assemble actin is not fully understood. BimA homologues of divergent N-terminal amino acid sequence exist in the closely related species *B. mallei* and *B. thailandensis*[8]. These proteins vary in their composition and number of actin-binding WH2 domains, the presence of proline-rich motifs, PDAST repeats and Arp2/3-binding CA domains implying that different *Burkholderia* species have evolved distinct strategies of actin-based motility[6, 8-9]. For example only *B. thailandensis* BimA sequesters Arp3, consistent with the presence of a unique CA domain[9a]. Despite the variation in sequence both *B. mallei* and *B. thailandensis* BimA proteins can functionally substitute for the actin-based motility defect of a *B. pseudomallei bimA* mutant[8]. Similarly, BimA proteins from *B. pseudomallei* and *B. mallei* can restore actin-based motility to a *B. thailandensis*

bimA mutant[9b, 10]. In *B. mallei* and *B. pseudomallei*, *bimA* gene expression is co-regulated with the virulence-associated Type VI Secretion System cluster through a two-component sensor-regulator VirAG which senses host cytosolic glutathione levels[11].

In common with other bacterial pathogens capable of actin-based motility, the Arp2/3 complex can be detected in *B. pseudomallei* actin-rich tails[12]. However, we have previously shown that *B. pseudomallei* BimA does not require the Arp2/3 complex to promote actin polymerisation *in vitro*[4, 9a], a finding confirmed recently by Benanti *et al*.[9b] and supported by observations by Lu and colleagues in which Arp2/3 depletion failed to inhibit *B. pseudomallei* actin-based motility[10]. Taken together with the findings that N(neural)-WASP and the vasodilator-stimulated phosphoprotein (VASP) are not required for actin-based motility of *B. pseudomallei*[12], and that actin-based motility is insensitive to overexpression of the WA fragment of Scar1 (which inhibits actin-based motility of *L. monocytogenes*, *S. flexneri* & *R. conorii*)[12], it may be inferred that *B. pseudomallei* employs a distinct mechanism for intracellular motility to other pathogens. Indeed it has recently been suggested that BimA mimics cellular Ena/VASP proteins promoting the polymerisation and elongation of actin tails[9b].

In a similar manner described for the characterisation of host cell proteins in the actin tails of *Listeria monocytogenes*[13], we have utilised an affinity purification approach to identify the cellular proteins recruited to *B. pseudomallei* under conditions that promote actin assembly *in vitro*. This relied on overexpression of VirAG to drive surface expression of BimA in *B. pseudomallei* and pulldown of host proteins from a murine splenic extract. Using this approach we have identified a number of proteins common to both the actin-rich tails of *L. monocytogenes* and *B. pseudomallei*, together with a number of proteins uniquely associated with the actin tails of *B. pseudomallei*. Association of a subset of these proteins with BimA-expressing bacteria was validated by immunoblotting. Confocal microscopy confirmed the recruitment of the cellular cytoskeletal scaffold protein Ras GTPase-activating-like protein (IQGAP1) to the actin tails of *B. pseudomallei* in infected cells. Using siRNA-mediated knockdown we also demonstrate that IQGAP1 plays a role in regulating the actin density and tail length of *B. pseudomallei* actin tails in infected cells.

4

1
2
3
4
5
6
7
8
9
10
11
12
13
14
15
16
17
18
19
20
21
22
23
24
25
26
27
28
29
30
31
32
33
34
35
36
37
38
39
40
41
42
43
44
45
46
47
48
49
50
51
52
53
54
55
56
57
58
59
60

Materials and methods

Bacterial strains

Burkholderia pseudomallei strain 10276 (NCTC 10276) was isolated from a British seaman suffering from the chronic form of melioidosis after likely exposure in Bangladesh[14]. Strain 10276 and our *bimA* insertion mutant[4] were transformed with pBHR2-*virAG*[11b] (a kind gift from Paul Brett and Mary Burtnick, University of South Alabama, US) by electroporation[15] to give strains 10276 pBHR2-*virAG* and 10276 *bimA*::pDM4 pBHR2-*virAG*. Bacteria were cultured in Luria Bertani broth supplemented with appropriate antibiotics at 37°C with shaking for ~16 hours.

To generate a *bimA* deletion mutant, approximately 400 base pairs immediately upstream of the *bimA* gene (annotated as BPSS1492 in the reference *B. pseudomallei* K96243 genome) was amplified using primers P1 (ATATATCTCGAGACCCGACACGCCGTGGACAGAA) and P2 (ATATATGGGCCCCATATCGATTGGCAGTGCCGT) using GC advantage polymerase (Takara Biotech Europe, Saint-German-en-Laye, France) following the manufacturer's instructions. Genomic DNA from strain NCTC 10276 was used as template. The PCR product was digested with *Xho*I and *Apa*I and ligated into similarly digested pDM4, an oriR6K *sacB* positive-selection suicide replicon[16]. The resulting plasmid was designated pDM4-*bimA*1. Next, approximately 540 base pairs downstream of the *bimA* gene was amplified from 10276 genomic DNA by PCR using primers P3 (ATATATGGGCCCTAAGCACCCGCAAACCCCCCCGGGCATC) and P4 (ATATATAGATCTCAGGCTGCAGAACGCAGGCT). The PCR product was restricted with *Apa*I and *Bgl*II prior to ligation with similarly digested pDM4-*bimA*1. The resulting plasmid was designated pDM4-Δ*bimA*.

Construction of the *B. pseudomallei* mutant was performed according to the method described by Logue *et al.*[17]. Briefly, pDM4-Δ*bimA* was introduced into *B. pseudomallei* strain NCTC 10276 by conjugation from *E. coli* S17.1λpir. Colonies were selected on LB agar plates containing 50μg/ml kanamycin and 50 μg/ml chloramphenicol. Colonies were screened by PCR with P1 and P4 primers to detect integration of the plasmid. A *B. pseudomallei* 10276 pDM4-Δ*bimA* merodiploid was next cultured in the absence of selection for the integrated plasmid then plated on LA plates lacking NaCl and containing 15% (w/v) sucrose to positively

5

select for a second recombination event involving excision of pDM4 and the *bimA* allele. Resulting colonies were then screened by PCR using flanking primers BimA screen 1 (GATGTCGCCGACGAAAGCAG) and BimA screen 2 (AGTGGGCGCGATTCTCGCGGCT) for the presence of a truncated *bimA* gene (of around 1Kb) instead of the full length gene (of around 2.5Kb). The resulting *bimA* deletion mutant was designated 10276 Δ*bimA*.

Preparation of murine splenic lysates

Spleens were harvested from BALB/c or VM mice at post mortem. Spleens were rinsed in ice-cold polymerisation buffer (10mM Tris pH 7.5, 50mM KCl, 2mM $MgCl_2$). 1ml of ice-cold polymerisation buffer supplemented with protease and phosphatase inhibitors (1mM phenylmethanesulfonyl fluoride (PMSF), 2mM Na_2VO_3, 2mM NaF, 2mM Na pyrophosphate, 1μg/ml aprotinin, 10μg/ml leupeptin, 1μg/ml pepstatin A) was added per spleen and the tissues homogenised. Supernatants were clarified by ultracentrifugation at 100,000x g for 2 hours at 4^oC. The clarified supernatants were carefully pipetted and stored at -70^oC between assays. The protein concentration of the murine splenic lysate was determined to be ~7mg/ml using a bicinchoninic acid protein assay kit (Thermo Fisher Scientific, Cramlington, UK).

Affinity purification of *Burkholderia*-associated proteins

Interacting proteins were isolated essentially as described by David *et al.*[13a] with some modifications. Approximately 1 x 10^9 bacteria were pelleted and suspended in 1.5ml murine splenic lysate supplemented with 5mM ATP and 30mM creatine phosphate. Bacteria were incubated for 1 hour at 37^oC with gentle agitation. Bacteria were washed gently with 1ml ice-cold 10mM PIPES pH7.25 containing 40mM KCl, 5mM ATP and 5mM $MgCl_2$. Interacting proteins were eluted from the bacterial surface using 0.5ml 10mM PIPES pH7.25 containing 1M KCl, 5mM ATP and 5mM $MgCl_2$. After repeating the elution, the eluate was filter-sterilised by passing through a 0.2μm membrane filter before concentrating the proteins using 30 μl StrataClean resin (Agilent Technologies UK Ltd., Stockport, UK). Resin were suspended in Laemmli sample treatment buffer containing 2% (v/v) β-mercaptoethanol. After incubation at 95^oC for 10 minutes, samples were separated by SDS-PAGE using a 4-15% gradient gel. After electrophoresis bands were stained using a SilverSnap kit following

the manufacturer's instructions (Thermo Fisher Scientific, Cramlington, UK). Bands were excised and subjected to LC-MS/MS.

LC-MS/MS

Gel slices were destained with 15mM potassium ferricyanide/50mM sodium thiosulphate for 5 minutes, reduced with 10mM DTT/100mM ammonium bicarbonate for 30 minutes and alkylated with 55mM iodoacetamide/100mM ammonium bicarbonate for 20 minutes. Gel slices were washed with 100mM ammonium bicarbonate and dehydrated with 100% (v/v) acetonitrile. Proteins were digested with 6 ng/ml trypsin/50mM ammonium bicarbonate for 5 hours at 37^oC and peptides were extracted in 1% (v/v) formic acid/2% (v/v) acetonitrile followed by 50% (v/v) acetonitrile. LC-MS/MS analysis of peptides were performed on a nanoAcquity UPLC system coupled to Q-Tof Premier Mass Spectrometer (Waters Corporation, Milford, Massachusetts, USA). Tryptic peptides were desalted and concentrated on a C_{18} TRAP column (180μm x 20mm, 5μm Symmetry, Waters), for 3 minutes at 10μl/ minute and resolved on a 1.7μm BEH 130 C_{18} column (100μm x 100mm, Waters Corporation) using a Waters Corporation nanoAcquity UPLC. Peptides were eluted at 400 nl/ minute with a linear gradient of 0-50% (v/v) acetonitrile/ 0.1% (v/v) formic acid over 30 minutes, followed by 85% (v/v) acetonitrile/ 0.1% (v/v) formic acid for 7 minutes. Eluted peptides were analysed on a Q-Tof Mass Spectrometer in 'data directed' acquisition mode, where an MS survey scan was used to automatically select double and multiple charged peptides for further MS/MS fragmentation. From each survey scan up to three of the most intense peptides were selected for fragmentation. MS/MS collision energy was dependent on precursor ion mass and charge state. A reference spectrum was collected every 30 seconds from the Glu-fibrinopeptide B (785.8426 m/z), introduced via a reference sprayer.

The raw mass spectral data was processed with ProteinLynx Global Server 2.3 (Waters Corporation) to generate peaklist files. The mass accuracy of the spectra was further corrected by using the reference spectra from Glu-fibrinopeptide B. The resulting peaklist files were searched against a locally installed protein sequence database (5855 entries) of the *B. pseudomallei* reference strain K96243 and mouse International Protein Index (IPI) database[18] using Mascot ver. 2.3 (Matrix Science, London, UK). Precursor and fragment ion mass tolerance were set to +/- 100 ppm and +/- 0.1 Da respectively. Trypsin specificity was

7

used for allowing up to one missed cleavage. Carbamidomethylation of cysteines and oxidation of methionines were selected as fixed and variable modifications respectively. The interpretation and presentation of MS/MS data was performed according to published guidelines[19].

Immunoblotting of bacterial and affinity-purified host proteins

Protein samples were denatured by heating to 95°C for 5 minutes in Laemmli buffer containing a final concentration of 1% (v/v) β-mercaptoethanol. Proteins were resolved by SDS-PAGE and transferred to PVDF or nitrocellulose membranes using a semi-dry transfer system (Bio-Rad, Hemel Hempstead, UK). Membranes were then blocked and incubated sequentially with primary antibodies at a concentration of 0.5-1 µg/ml followed by species-specific antibodies conjugated with horseradish peroxidase (for standard ECL detection, GE Healthcare, Chalfont St. James, UK) or fluorescently labelled secondary antibodies (α-rabbit IgG DyLight[800], Cell Signalling Technology, Leiden, The Netherlands), followed by detection using a Biosciences Odyssey infrared imaging system (LI-COR Biosciences, Cambridge, UK). Primary antibodies used in immunoblotting were: mouse anti-BimA monoclonals AF8, FB5 and FG11[4]; rabbit anti-BopE[20]; mouse anti-*B. pseudomallei* capsule (a kind gift from Dstl, Porton Down, UK[21]); goat anti-actin (Source Bioscience, Nottingham, UK); goat anti-IQGAP1 (Abcam, Cambridge, UK); rabbit anti-IQGAP1 (Insight Biotechnology, Wembley, UK); rabbit anti-vinculin (Source Bioscience, Nottingham, UK); rabbit anti-HSP90 (Source Bioscience, Nottingham, UK) and rabbit anti-L-Plastin (Source Bioscience, Nottingham, UK).

Cell infection, siRNA knockdown and fluorescence microscopy

HeLa cells were cultured on sterile glass coverslips and infected at a multiplicity of infection (MOI) of ~100 essentially as described in Sitthidet *et al*.[6]. At the indicated time points post-infection coverslips were rinsed with phosphate-buffered saline (PBS) and incubated for a minimum of 16 hours in PBS containing 4% (w/v) paraformaldehyde before staining for confocal microscopy. Coverslips were treated with 0.5% (v/v) Triton-X100 in PBS for 15 minutes to permeabilise infected cells, blocked for 30 minutes in 0.5% (w/v) BSA in PBS and then sequentially incubated in 0.5µg/ml primary and fluorescently labelled secondary antibodies or cell stains as indicated in figure legends. Primary antibodies used in

8

fluorescence microscopy: mouse anti-BimA AF8, FB5 and FG11[4]; mouse anti-*B. pseudomallei* lipopolysaccharide (LPS) (Camlab, Cambridge, UK); rabbit anti-IQGAP1 (Insight Biotechnology, Wembley, UK). Actin filaments were stained with Phalloidin Alexa Fluor[488] (Life Technologies Ltd., Paisley, UK). Images were captured using a Leica Microsystems (Milton Keynes, UK) LSM710 confocal scanning microscope and Zen 2011 software (Carl Zeiss Ltd., Cambridge, UK).

To reduce expression of IQGAP1 in HeLa cells, approximately 30,000 cells plated per well of a 24-well tissue culture plate were transfected with 6pmol Silencer Select IQGAP1 siRNA duplex (Life Technologies Ltd., Paisley, UK) using Lipofectamine RNAiMax (Life Technologies Ltd., Paisley, UK) essentially as described by the manufacturer's instructions. Cells were lysed at 72 hours post-transfection to detect IQGAP1 knockdown by immunoblotting. Whilst optimising conditions for IQGAP1 knockdown cells transfected with MISSION negative control siRNA (Sigma-Aldrich, Dorset, UK) were used for reference. For infection experiments, IQGAP1 siRNA-transfected cells were incubated for 56 hours prior to infection with *B. pseudomallei* strain 10276. Cells were infected at an MOI of ~100 for a further 16 hours before fixation and staining for confocal microscopy analysis.

Images representing maximal projection z-stacks were captured using identical laser settings from 3 independent experiments and analysed using Image J software (http://imagej/nih.gov/ij/). The maximal calliper function was used to calculate the length of tails and the corrected total cell fluorescence (CTCF) formula to determine the intensity of actin staining throughout each tail. Data from a total of 100 tails from each condition were collated and analysed using a student t-test in GraphPad Prism.

Yeast 2 Hybrid

A fragment of the *bimA* gene encoding amino acids 54 to 455 of the BimA protein (capable of binding and polymerising actin *in vitro*) was cloned into pGBKT7 (Clontech, Saint-Germain-en-Laye, France) to express an in-frame fusion protein with the GAL4 DNA-binding domain. The *bimA* gene was amplified by PCR from 10276 genomic DNA using primers F-BimA (GCGCGCCATATGAATCCCCCCGAACCGCCGGGC) and R-BimA (GCGCGCGAATTCTTAGCGCGCGGTGTCGGTG). The product was purified, digested with *Nde*I and *Eco*RI, and ligated into similarly digested vector to give pGBKT7-*bimA*. This plasmid was

9

introduced into *Saccharomyces cerevisiae* strain AH109 using a standard lithium acetate mediated transformation protocol outlined in the Matchmaker GAL4 Yeast Two Hybrid System 3 handbook (Clontech, Saint-Germain-en-Laye, France) with selection on SD media lacking tryptophan (Clontech, Saint-Germain-en-Laye, France), to give strain AH109 pGBKT7-*bimA*. The *iqgap1* gene was amplified by PCR from HeLa cell cDNA (AMS Biotechnology Ltd, Abingdon, UK) using primers F-IQGAP1 (TTTTCATATGATGTCCGCCGCAGACGAG) and R-IQGAP1 (TTTTCTCGAGTTACTTCCCGTAGAACTTTTTGTTGA). Similarly the *actb* gene was amplified by PCR from HeLa cell cDNA using primers F-actin (TTTTCATATGATGGATGATGATATCGCCG) and R-actin (TTTTCTCGAGCTAGAAGCATTTGCGGTGG). PCR products were purified, digested with *Nde*I and *Xho*I, and ligated into similarly digested pGADT7 (Clontech, Saint-Germain-en-Laye, France) to create pGADT7-*iqgap1* and pGADT7-*actin*, encoding in-frame fusion proteins with the GAL4 activation domain. All plasmids were verified by sequencing prior to transformation into AH109 strains and selection on SD media lacking leucine. The pGADT7-*iqgap1* and pGADT7-*actb* plasmids were separately introduced into AH109 pGBKT7-*bimA* by lithium acetate with selection on SD media lacking leucine and tryptophan (DDO: Double Drop Out media, Clontech, Saint-Germain-en-Laye, France) to give strains AH109 pGBKT7-*bimA* pGADT7-*iqgap1* and AH109 pGBKT7-*bimA* pGADT7-*actin*.

To identify protein: protein interactions, single yeast colonies from DDO agar plates were suspended in 20μl water and 5μl dotted onto SD agar plates lacking leucine, tryptophan, adenine and histidine (QDO: Quadruple Drop Out) supplemented with 20μg/ml X-α-galactosidase. Plates were incubated at 30°C for 24 hours before observing the appearance of the colonies. The strains AH109 pGBKT7-*bimA* pGADT7-*iqgap1* and AH109 pGBKT7-*bimA* pGADT7-*actin* were tested alongside yeast strains transformed with positive and negative control vectors (pGADT7-T antigen pGBKT7-p53 and pGADT7-T antigen pGADT7-Lamin C respectively) supplied with the Matchmaker GAL4 Y2H System 3 (Clontech, Saint-Germain-en-Laye, France).

10

Results

Engineering a *Burkholderia pseudomallei* strain that constitutively expresses BimA *in vitro*

BimA (BPSS1492), a predicted Type V autotransporter protein of *Burkholderia pseudomallei*, is required for actin-based motility of the bacterium in the cytosol of infected cells[4, 6]. We have found that BimA expression is below the limit of detection in bacteria cultured in common laboratory media (Figure 1a) but detectable from 6 hours post-infection by immunoblotting infected cell lysates with antibodies specific to BimA[4] (Figure 1b). The presence of intracellular bacteria in all samples was confirmed by immunoblotting with antibody reactive to the *B. pseudomallei* capsule[21]. In the closely related species *B. mallei*, *bimA* gene transcription and BimA protein expression is positively regulated by a two-component system, VirAG, encoded adjacent to the *bimA-E* genes on chromosome 2[11b]. In order to induce BimA expression in LB-cultured bacteria we therefore introduced the pBHR2-*virAG* plasmid constitutively expressing the *B. mallei virAG* genes[11b] into strain NCTC 10276[14] or our *bimA* insertion mutant giving strains 10276 pBHR2-*virAG* and 10276 *bimA*::pDM4 pBHR2-*virAG*. The VirA and VirG proteins of *B. mallei* and *B. pseudomallei* share 99.4% and 99.6% identity respectively and introduction of the pBHR2-*virAG* plasmid into these strains resulted in expression of BimA protein in wild-type bacteria cultured in laboratory medium (Figure 1a). Protein loading was confirmed using an antibody against the *B. pseudomallei* Bsa Type III Secretion System effector protein BopE[20]. Localisation of BimA on the surface of the 10276 pBHR2-*virAG* strain was confirmed by confocal microscopy of intact bacteria (data not shown).

Isolation of candidate host cell proteins involved in actin-based motility of *B. pseudomallei*

Having established an *in vitro* system in which *B. pseudomallei* bacteria were expressing BimA, we set out to identify host cell proteins that associated with 10276 pBHR2-*virAG* (BimA-expressing bacteria) and common bacterial proteins released from the bacterial surface following elution from 10276 pBHR2-*virAG* and 10276 *bimA*::pDM4 pBHR2-*virAG*. Bacteria were incubated with murine splenic lysates under conditions that promote BimA: actin binding and actin polymerisation[4] and interacting proteins eluted and concentrated for SDS-PAGE. Following silver staining gel slices were excised and subjected to in-gel trypsin

11

digestion, extraction and LC-MS/MS analysis. A representative silver stained gel is shown in Figure 2. Spectra were then separately searched against the mouse International Protein Index (IPI) database[18] and an 'in-house' *B. pseudomallei* K96243 protein database to obtain protein identifications. Data were collected for 3 independent experiments with both bacterial and host cell proteins identified in the eluted proteins.

We sought to identify host cell proteins that were solely associated with, or identified at a higher frequency with, the BimA-expressing bacteria 10276 pBHR2-*virAG* compared to the *bimA* mutant strain 10276 *bimA*::pDM4 pBHR2-*virAG*. Spectra were screened against the mouse IPI database[18] and protein identifications assigned when the proteins were identified in at least two of the three biological replicates. From this analysis a set of 30 host proteins were isolated (Table 1). In contrast to a previous study on the proteome of *L. monocytogenes* actin tails[13b], there was a notable lack of microtubule components, intermediate filaments or myosins. The most abundant and commonly isolated proteins recruited in a VirAG-dependent manner were those of the actin family, consistent with the known actin-binding activity of BimA[4]. Several of the proteins are associated with areas of dynamic actin assembly such as membrane ruffles and cell junctions, or acting as scaffolds to integrate signalling complexes. A selection of host cell proteins recruited by BimA-expressing bacteria contained FERM domains, which are known to localise at the interface between the cytoskeleton and the plasma membrane. The scaffold proteins Talin, 14-3-3 protein zeta/delta and IQGAP1 were identified, as were components of the Arp2/3 complex (specifically subunits 1b, 2 and 4), previously described as being in the actin tails of *B. pseudomallei*[12]. In addition to actin, we identified several F-actin binding proteins implicated in stabilising F-actin networks through bundling and cross-linking activities (α-actinins 1 and 4, Filamin A, Spectrin/ fodrin, Vinculin, Tropomyosin, Plastin-2/ L-Plastin, Transgelin), several F-actin capping proteins (Spectrin/ fodrin, ERM proteins, Macrophage capping protein, CapZ) and an actin-depolymerising factor (ADF) in the form of cofilin. We also identified the proteins WD repeat-containing protein 1 (AIP1) and serine/ threonine phosphatase 2A, known regulators of cofilin activity.

Several *B. pseudomallei* proteins were consistently identified in eluates from both wild-type and *bimA* mutant bacteria (Table 2), including the Type VI secreted protein Hcp (BPSS1498), a number of chaperone proteins and proteases. A number of the *B.*

pseudomallei proteins identified in this study have previously been identified in the *B. pseudomallei* outer membrane proteome[22], the total secretome[23] or as surface proteins by surface labelling approaches[24], including the molecular chaperones GroEL (BPSL2697 and BPSS0477), GroES (BPSL2698), DnaK (BPSL2827) and the transcription/ translation factors Tuf (BPSL3215) (labelled OM in Table 2). Several have also been shown to be recognised by the sera of convalescent melioidosis patients (labelled I in Table 2)[24-25]. The remainder of proteins ranged in function from metabolic enzymes involved in glycolysis, amino acid metabolism and the TCA cycle to RNA polymerase subunits. These may represent particularly abundant proteins of the bacteria released upon cell lysis or proteins contained within outer membrane vesicles (OMVs). OMVs have recently been reported to have protective efficacy against pulmonary melioidosis and *B. pseudomallei*-induced sepsis[26], however a proteomic analysis of the contents of such OMVs has yet to be described.

Validation of the dataset

The dataset described in Table 1 was validated by immunoblotting of independently-generated samples for a subset of host cell proteins. An equal volume of eluted protein generated from identical treatment of similar numbers of bacteria was probed in each instance. Proteins that were identified in all 3 experiments, with high MASCOT scores, and were novel when compared to proteins involved in *Listeria* or *Shigella* actin-based motility were confirmed (HSP90 and IQGAP1) (Figure 3). We also chose to validate one of the proteins identified in only 2 experiments with a moderate MASCOT score (vinculin) or identified in all 3 experiments with a low MASCOT score (L-Plastin) (Figure 3). As a positive control the recruitment of actin to BimA-expressing bacteria was also verified (Figure 3). All chosen targets were detected in murine splenic lysate and samples derived from bacteria expressing BimA *in vitro* (10276 pBHR2-*virAG*), and were absent from those samples lacking BimA (10276 *bimA*::pDM4 pBHR2-*virAG*).

IQGAP1 is present in actin tails formed by intracellular *B. pseudomallei*

The Ras GTPase-activating-like protein IQGAP1 is a ubiquitously expressed scaffold protein that integrates multiple host signalling pathways including actin cytoskeleton dynamics, cell cycle and cell adhesion. To date this protein has not been shown to be

13

involved in the actin-based motility of intracellular bacteria, although it has been shown to be involved in entry of *Salmonella* into host cells and for actin pedestal formation of attaching and effacing *E. coli* pathotypes to the apical surface of cells (reviewed by Kim *et al.*[27]). Our data implied that in contrast to *Listeria* and other pathogens that display actin-based motility, IQGAP1 may be a component of *B. pseudomallei* actin tails. Indeed this was supported by immunocytochemistry and confocal microscopy which revealed the presence of IQGAP1 throughout the tails of *B. pseudomallei* 10276 at 16 hours post-infection of HeLa cells (Figure 4(a)-(c)). In agreement with a recent report by Benanti *et al.*[9b], we could also elucidate the architecture of the *B. pseudomallei* actin tail by fluorescent actin staining coupled with confocal microscopy, albeit at low resolution (Figure 4(d)). The tails consisted of loosely bundled F-actin filaments reminiscent of those described for certain *Rickettsia* species that rely on the formin-like Sca2 autotransporter for actin polymerisation[28].

Yeast 2 Hybrid analysis detects a direct interaction between BimA and actin but not IQGAP1

Whilst IQGAP1 could readily be detected in the actin tails of all bacteria displaying actin-based motility in infected cells, we sought to determine if this is through direct interaction with the BimA protein using a Yeast 2 Hybrid approach. The Yeast 2 Hybrid assay is a widely utilised and sensitive molecular genetic approach to detect even weak or transient protein: protein interactions *in vivo*. It relies on the modular nature of transcriptional trans-activators where the DNA-binding and activation domains can be physically separated and expressed as fusions with proteins of interest. If the proteins interact they bring the DNA-binding and activation domains into close proximity thereby resulting in transcription of certain reporter genes. In our Yeast 2 Hybrid system the reporter genes for histidine and adenine biosynthesis (which allow growth on media lacking these two amino acids) and α-galactosidase (which produces blue colonies on media containing X-α-Gal substrate) are utilised. We have expressed amino acid residues 54 to 455 of the BimA protein as a DNA-binding protein fusion protein in the reporter yeast strain AH109 pGBKT7-BimA. When β-actin is also expressed in this strain as an activation domain fusion protein (AH109 pGBKT7-BimA pGADT7-actin), the yeast generates blue colonies on media containing X-α-Gal substrate but lacking leucine, tryptophan, adenine and histidine (QDO) (Figure 5), indicating

14

an interaction between these two proteins as we have previously described[4]. Conversely, introduction of a vector expressing IQGAP1 as an activation domain fusion protein into the BimA yeast strain (AH109 pGBKT7-BimA pGADT7-IQGAP1) resulted in growth of the yeast strain on QDO media, however the colonies remained white even after extended incubation times (Figure 5). Growth on selective media in the absence of detectable α-galactosidase activity indicates that these two proteins do not directly interact with each other. Growth under these circumstances can be attributed to a low level of intrinsic *trans*-activation in yeast strains harbouring the pGBKT7-BimA plasmid as shown in Figure 5.

Consistent with the Yeast 2 Hybrid data presented in Figure 5, we were unable to detect a direct interaction between BimA and IQGAP1 by conventional pulldown assay using affinity-purified glutathione S-transferase (GST)-BimA$_{54-455}$ and maltose-binding protein (MBP)-IQGAP1 fusion proteins expressed by *E. coli* under conditions previously used to detect the direct interaction of actin with BimA[4] (data not shown).

Effect of IQGAP1 knockdown on actin density and length of BimA-induced actin tails

Given the presence of IQGAP1 in the tails of *B. pseudomallei* in infected cells we next utilised an IQGAP1 siRNA approach to determine the functional relevance of this host cell protein in *B. pseudomallei* actin-based motility. Transfection of Silencer Select siRNA against IQGAP1 into HeLa cells consistently resulted in efficient knockdown of around 70% as assessed by IQGAP1 immunoblotting (Figure 6a and b). Following infection of siRNA knockdown cells and control non-transfected cells, over 2000 bacteria were imaged from each infected cell type across 3 biological replicates. There was no significant difference in the proportion of tailing bacteria in either cell type under the assay conditions used (~42%). It was evident that bacteria could still form actin tails in the knockdown cells however this may be a result of the residual IQGAP1 expression in the cells, or compensation by the related IQGAP proteins IQGAP2 or IQGAP3 which are also expressed in this cell type.

Using Image J software we next measured the length and actin density of tails as described in the Methods section. 100 tails from control and siRNA transfected HeLa cells across 3 biological replicates were analysed. The data showed a statistically significant increase in overall tail length (p=0.0033) with concomitant decrease in actin density (p=0.0001) in IQGAP1 knockdown cells compared with control cells (Figure 6c and d). In cells

15

with reduced levels of IQGAP1 tails were significantly longer with a mean length of 20.5µm compared to a mean length of 14.8 µm in control cells (Figure 6c). Although longer in length the actin density of tails generated in IQGAP1 knockdown cells was lower with a mean signal of 1036.0 A.U. compared to a mean signal of 2522.4 A.U. measured for tails in control cells.

Discussion

Burkholderia pseudomallei is a facultative intracellular bacterium capable of escape from the endocytic vacuole into the cytosol of host cells. In common with several other bacteria, namely *Listeria monocytogenes*, *Shigella flexneri*, *Mycobacterium marinum* and several *Rickettsia* spp., it is capable of harnessing cellular actin to promote its movement within and between host cells by actin-based motility. It is clear that these bacteria have evolved several independent mechanisms to utilise cellular actin and accessory proteins for actin-based motility. For example *L. monocytogenes* expresses ActA, a protein which recruits the host cell Arp2/3 complex to its surface where it directly interacts with actin and stimulates its polymerisation[29]. Conversely certain rickettsial species express Sca2, a protein which acts through functional mimicry of eukaryotic formins[28]. We have previously characterised the *B. pseudomallei* encoded protein required for actin-based motility. Known as BimA, this predicted Type V auto-transporter protein is expressed on a single pole of the bacterium where it recruits cellular actin and stimulates its polymerisation to mediate intracellular movement[4, 6]. We and others have shown that this protein can stimulate actin polymerisation *in vitro* in a manner that is independent of other host cell factors such as the Arp2/3 complex[4, 9]. Despite localisation of Arp2/3 components to the actin-rich tails of *B. pseudomallei* in infected cells[12], tail formation does not require the activity of this cellular actin nucleation complex since it can be observed in cells depleted of Arp2/3[10]. Whilst it is known that actin-based motility of *B. pseudomallei* does not require Arp2/3, the potential involvement of other cellular factors is unclear.

Here we have used an *in vitro* affinity approach to identify cellular factors recruited to BimA over-expressing bacteria under actin polymerising conditions. We report the identification of 30 cellular proteins, including actin, actin-depolymerising factor and capping protein, the minimal requirement for polymerisation in the presence of a bacterial actin polymerisation factor *in vitro*[30]. The identification of vinculin and α-actinin is

16

corroborated by the work of Breitbach *et al*. who demonstrated the presence of these proteins in *B. pseudomallei* actin tails by immunofluorescence microscopy[12]. Whilst α-actinin is commonly detected in the tails of bacteria that display actin-based motility, vinculin has been reported to be absent from *R. rickettsii* tails[31].

In comparison to previous studies, it was notable that our dataset lacked any microtubules, intermediate filaments or myosins that were shown to be present in *Listeria* tails[13b], or VASP or profilin, which have been shown to be components of *R. rickettsia* actin tails[31] Two proteins that have not previously been associated with actin-based motility of intracellular pathogens, HSP90 and IQGAP1, were identified in this analysis and the presence of IQGAP1 detected in actin-rich tails formed by *B. pseudomallei* in HeLa cells. IQGAP1 is a ubiquitously expressed scaffold protein that integrates numerous signalling pathways and regulates multiple cellular processes. Involved in *Salmonella* Typhimurium host cell invasion and *Chlamydophila pneumoniae*-induced vascular smooth cell migration, IQGAP1 has also been implicated in the adhesion of EPEC to the cell surface and viral trafficking and replication of Mu-MuLV (reviewed in Kim *et al*.[27]). IQGAP1 has been shown to interact directly with the EPEC Ibe and Tir proteins and Salmonella T3SS effector protein SseI, although the yeast 2 hybrid and pulldown results are not consistent with a direct interaction between IQGAP1 and BimA. Indeed, the finding that the protein localises along the length of the actin-rich tail in *B. pseudomallei* infected tails, together with reports that IQGAP1 is an actin-binding protein, suggests it is recruited indirectly through its interaction with actin filaments[32]. Furthermore we demonstrate that IQGAP1 plays a functional role in organising the architecture of the actin tails formed by *B. pseudomallei*. Indeed siRNA mediated knockdown resulted in a significant lengthening of the tails concomitant with a reduction in the actin density. This warrants further investigation, as does the role of the other validated and candidate host cell proteins in actin-based motility of this fascinating bacterial pathogen.

Conclusion

We have demonstrated a hitherto unknown role for the cellular protein IQGAP1 in modulating the length and actin density of actin tails induced by the intracellular bacterial pathogen *Burkholderia pseudomallei*.

17

Statement on Dual Use Research of Concern

The work described in this manuscript was undertaken in the United Kingdom through funding obtained from UK sources and in strict accordance with UK Health and Safety Executive (HSE) guidance. Our work in relation to genetic modification has been extensively reviewed both by our own University of Edinburgh Biosafety Unit, the HSE and by the UK Counter Terrorism and Security Agency. The genetically modified *B. pseudomallei* strains described in this paper do not constitute a US Government Dual Use of Research Concern since these modifications do not enhance the pathogenicity of the micro-organism, do not interfere with immunity or immunization strategies, do not confer resistance to useful prophylactic or therapeutic agents and do not alter the transmissibility, host range or tropism of the pathogen.

1
2
3
4
5
6
7
8
9
10
11
12
13
14
15
16
17
18
19
20
21
22
23
24
25
26
27
28
29
30
31
32
33
34
35
36
37
38
39
40
41
42
43
44
45
46
47
48
49
50
51
52
53
54
55
56
57
58
59
60

Figure legends

Figure 1: *Burkholderia pseudomallei* **BimA expression is not constitutive and can be induced by expression of VirAG** *in trans*. (a) Western blot analysis of BimA expression in whole cell lysates of bacteria cultured in LB overnight at 37°C. Bacterial lysates were probed for BimA and BopE (as a protein loading control) using specific antibodies, and show that BimA is not expressed by wild-type *B. pseudomallei* under standard culture conditions. Expression *in trans* of the two component regulator VirAG results in BimA expression. Note that approximately 10-fold more 10276 and *bimA*::pDM4 bacteria (than their p*virAG*-containing counterparts) were loaded onto the protein gel for analysis. (b) Western blot analysis of RAW cells infected with wild-type *B. pseudomallei* and a *bimA* mutant at an MOI of 100 at 3, 6 and 8 hours post-infection. Lysates were probed for BimA and *Burkholderia* capsule (as a protein loading control) using specific antibodies and indicate detection of BimA in lysates at the later time points post-infection.

Figure 2: Host cell and bacterial proteins are eluted from the surface of *B. pseudomallei* **strains incubated with murine splenic lysate.** A representative silver stained SDS-polyacrylamide gel showing the profile of proteins eluted from 10276 pBHR2-*virAG* and 10276 *bimA*::pDM4 pBHR2-*virAG* bacteria incubated with murine splenic lysates. The abundant presence of actin in the 10276 pBHR2-*virAG* sample is indicated by the arrow. Protein bands from samples from 3 independent experiments were processed for LC-MS/MS analysis.

Figure 3: Independent validation confirms the presence of a subset of host cell proteins in eluates from *B. pseudomallei* **strains incubated with murine splenic lysate.** Independent protein eluates from 10276 pBHR2-*virAG* and 10276 *bimA*::pDM4 pBHR2-*virAG* bacteria incubated with murine splenic lysates were prepared and immunoblotted to confirm the specific presence of IQGAP1, vinculin, HSP90 and L-plastin in the 10276 pBHR2-*virAG* samples. 5μg and 10μg of total splenic lysate were loaded as positive controls for the antibodies.

19

Figure 4: IQGAP1 is recruited to *B. pseudomallei* actin tails in infected HeLa cells. HeLa cells were infected with *B. pseudomallei* at an MOI of 100 and fixed at 16 hours post-infection for visualisation of actin tails by immunohistochemistry and confocal microscopy. Representative images of bacteria (blue) and actin (green) are shown in panel (a), and bacteria (blue) and IQGAP1 (red) in panel (b). The white arrows indicate areas of co-localisation of actin and IQGAP1 in bacterial tails. Panel (c) represents a merged image of (a) and (b). (d) illustrates the architecture of the actin tails, where the scale bar is 5μm.

Figure 5: BimA and IQGAP1 do not interact in a yeast two-hybrid assay. To identify protein: protein interactions, single yeast colonies from SD agar plates lacking leucine and tryptophan (DDO: <u>D</u>ouble <u>D</u>rop <u>O</u>ut) were suspended in 20μl water and 5μl dotted onto SD agar plates lacking leucine, tryptophan, adenine and histidine (QDO: <u>Q</u>uadruple <u>D</u>rop <u>O</u>ut) supplemented with 20μg/ml X-α-galactosidase. Plates were incubated at 30°C for 24 hours before observing the appearance of the colonies. The strains AH109 pGBKT7-*bimA* pGADT7-*iqgap1* (BimA X IQGAP1) and AH109 pGBKT7-*bimA* pGADT7-*actin* (BimA X actin) were tested alongside yeast strains transformed with positive and negative control vectors (pGADT7-T antigen pGBKT7-p53 and pGADT7-T antigen pGADT7-Lamin C, respectively). The blue colouration of the yeast indicates a direct interaction between the two proteins, as demonstrated by the positive control and BimA X actin strains. White colouration indicates a lack of interaction between the two proteins, as demonstrated by the negative control and BimA X IQGAP1 strains.

Figure 6: siRNA-mediated knockdown of IQGAP1 in HeLa cells affects *B. pseudomallei* tail morphology. (a) Western blot analysis of HeLa cell lysates from three independent experiments. IQGAP1 and actin (as a protein loading control) were detected in lysates prepared from cells treated only with transfection reagent (control) and cells transfected with 6pmol siIQGAP1 for 72 hours (IQGAP1 siRNA). (b) Quantitation of IQGAP1 protein levels in control and IQGAP1 siRNA cells indicates that IQGAP1 expression is reduced by ~70% in siRNA-treated cells. Control and IQGAP1 siRNA cells were infected with *B. pseudomallei* at an MOI of 100 and fixed at 16 hours post-infection for visualisation of actin tails by immunohistochemistry and confocal microscopy. Images were collected from three

20

independent experiments and tail length in μm (c) and actin density in A.U. of phalloidin

intensity (d) assessed using ImageJ software.

Table 1: Host cell proteins isolated from BimA-expressing *Burkholderia pseudomallei*.

Gene ID	Gene Name	Description	Protein Accession No.	Protein Score	# Unique Peptides	Notes
IPI00131138	***flna***	**Filamin A**	**Q8BTM8**	**104**	**32**	**Lm**
IPI00753793	*spna2*	Spectrin alpha chain/ fodrin alpha chain	P16546	176	50	Lm
IPI00319830	*spnb2*	Spectrin beta chain/ fodrin beta chain	Q62261	79	8	Lm
IPI00465786	*tln1*	Talin 1	P26039	91	8	Lm
IPI00467447	***iqgap1***	**IQ motif containing GTPase activating protein 1, IQGAP1**	**Q9JKF1**	**107**	**49**	
IPI00405227	*vcl*	Vinculin	Q64727	67	12	Lm
IPI00118899	***actn4***	**Alpha-actinin-4**	**P57780**	**109**	**31**	**Lm**
IPI00380436	*actn1*	Alpha-actinin-1	Q7TPR4	116	38	Lm
IPI00229080	*hsp90ab1*	Heat shock protein 90kDa alpha	Q71LX8	79	17	
IPI00169731	*fermt3*	Fermitin family homolog 3/ kindlin 3	Q8K1B8	55	1	
IPI00118892	***lcp1***	**Lymphocyte cytosolic protein 1/ plastin -2/ L-plastin**	**Q61233**	**58**	**3**	**Lm (T-plastin)**
IPI00338302	*pgm2*	Phosphoglucomutase-2	Q7TSV4	43	2	
*****	***ezr/msn/rdx***	**Ezrin/ Radixin/ Moesin****	******	**61**	**4**	**Lm (Ezrin)**
IPI00314748	*wdr1*	WD repeat-containing protein 1/ AIP1	O88342	61	2	Lm
IPI00110827	***acta1***	**Alpha actin**	**P68134**	**98**	**34**	**Lm**
IPI00125143	*arpc1b*	Actin-related protein 2/3 complex subunit 1b	Q91Z25	58	2	
IPI00473320	***actb***	**Beta actin-like protein**	**Q3U804**	**140**	**117**	**Lm**
IPI00874482	***actg1***	**Gamma actin**	**P63260**	**140**	**121**	**Lm**
IPI00110850	***actb***	**Beta actin**	**P60710**	**103**	**34**	**Lm**
IPI00277930	*capg*	Macrophage-capping protein	Q99LB4	96	6	
IPI00830701	*tpm1*	Tropomyosin 1	P58771	102	11	Lm
IPI00111556	*ppp2cb*	Serine/ threonine phosphatase 2A catalytic subunit	P62715	62	1	
IPI00111265	*capza2*	F-actin-capping protein subunit alpha-2	P47754	77	1	Lm
IPI00874728	*tpm2*	Tropomyosin 2	P58774	102	13	Lm

22

IPI00775844	*arpc2*	Actin-related protein 2/3 complex subunit 2	Q9CVB6	71	3	Lm
IPI00230044	*tpm3*	Tropomyosin 3	Q58E70	88	7	Lm
IPI00116498	*ywhaz*	14-3-3 protein zeta/delta	P63101	71	6	Lm
IPI00125778	***tagln2***	**Transgelin 2**	**Q9WVA4**	**69**	**2**	**Lm**
IPI00138691	***arpc4***	**Actin-related protein 2/3 complex subunit 4**	**P59999**	**51**	**5**	**Lm**
IPI00890117	*cfl1*	Cofilin-1	P18760	100	3	Lm

*Peptides matched ezrin (IPI00330862, P26040), moesin (IPI00110588, P26041) and radixin (IPI00308324, P26043)

List of murine proteins isolated either solely or at a higher frequency from eluates from BimA-expressing bacteria 10276 pBHR2-*virAG* compared to the *bimA* mutant strain 10276 *bimA*::pDM4 pBHR2-*virAG*. Proteins were assigned when peptides were isolated in at least 2 experiments, with a MASCOT score of at least 30, at least one rank 1 peptide, where the predicted mass of the protein matched the observed mass and where the reported cellular localisation was listed as cytoplasm or plasma membrane. Proteins highlighted in grey and shown in bold were isolated in all 3 experiments. Proteins are listed in order of molecular weight (highest to lowest) with 'Lm' in the Notes column denoting the identification of this protein in similar proteomic studies of *Listeria monocytogenes* tails.

Table 2: *Burkholderia pseudomallei* **proteins identified in the samples.**

Gene ID	Gene Name	Description	Protein Accession No.	Protein Score	# Unique Peptides	Notes
bpsl0779	*sucC*	Succinyl-CoA synthetase subunit beta	YP_107404.1	88	2	
bpsl1013	*ppc*	Phosphoenolpyruvate carboxylase	YP_107641.1	67	4	
bpsl1087	*htpG*	Heat shock protein 90	YP_107709.1	103	4	
bpsl1402	*tig*	Trigger factor	YP_108024.1	69	6	
bpsl1405	*lon*	ATP-dependent protease	YP_108027.1	96	6	
bpsl2192	*aceB*	Malate synthase	YP_108787.1	80	4	
bpsl2270	*eno*	Phosphopyruvate hydratase	YP_108866.1	128	3	
bpsl2305		Oligopeptidase A	YP_108901.1	117	2	
bpsl2697	*groEL*	Chaperonin GroEL	YP_109293.1	157	38	OM, I
bpsl2698	*groES*	Co-chaperonin GroES	YP_109294.1	169	8	I
bpsl2827	*dnaK*	Molecular chaperone DnaK	YP_109422.1	107	6	OM, I
bpsl2953	*tktA*	Transketolase	YP_109547.1	101	8	
bpsl3004	*rpmA*	50S ribosomal protein L27	YP_109599.1	109	2	
bpsl3196	*rpsE*	30S ribosomal protein S5	YP_109790.1	78	5	
bpsl3215	*tuf*	Elongation factor Tu	YP_109809.1	104	9	
bpsl3220	*rpoC*	DNA-directed RNA polymerase subunit beta'	YP_109814.1	102	23	
bpsl3221	*rpoB*	DNA-directed RNA polymerase subunit beta	YP_109815.1	117	22	
bpss0421	*rfbH*	Lipopolysaccharide biosynthesis protein (O-antigen-related)	YP_110445.1	45	1	I
bpss0879		Porin protein	YP_110888.1	83	2	OM, I
bpss0913		Methionine gamma-lyase	YP_110922.1	104	4	
bpss1356		Hypothetical protein	YP_111366.1	133	22	OM
bpss1498	*hcp*	Hypothetical protein (Type VI secretion system secreted protein Hcp)	YP_111505.1	112	14	
bpss1715	*gltA*	Type II citrate synthase	YP_111721.1	81	7	
bpss1722	*mdh*	Malate dehydrogenase	YP_111728.1	107	5	I
bpss1726	*acnA*	Aconitate hydratase	YP_111732.1	118	20	

25

1
2
3
4
5
6
7
8
9
10
11
12
13
14
15
16
17
18
19
20
21
22
23
24
25
26
27
28
29
30
31
32
33
34
35
36
37
38
39
40
41
42
43
44
45
46
47
48
49
50
51
52
53
54
55
56
57
58
59
60

List of *Burkholderia pseudomallei* proteins isolated from eluates from both 10276 pBHR2-*virAG* and 10276 *bimA*::pDM4 pBHR2-*virAG* bacteria. Proteins were assigned when peptides were isolated from both samples in at least 2 experiments, with a MASCOT score of at least 30, at least one rank 1 peptide and where the predicted mass of the protein matched the observed mass. Proteins highlighted in grey and shown in bold were isolated in all 3 experiments. In the Notes column, 'OM' indicates that the protein has previously been described as surface associated or a component of the *B. pseudomallei* outer membrane proteome[22, 24]. 'I' indicates the protein is recognised by recovering human melioidosis patient sera[24-25]. Proteins are listed in order of *B. pseudomallei* gene number with chromosome 1 encoded proteins (BPSLxxxx) listed first.

References

1. Wiersinga, W. J.; van der Poll, T.; White, N. J.; Day, N. P.; Peacock, S. J., Melioidosis: insights into the pathogenicity of *Burkholderia pseudomallei*. *Nature reviews. Microbiology* **2006,** *4* (4), 272-82.

2. Stevens, J. M.; Galyov, E. E.; Stevens, M. P., Actin-dependent movement of bacterial pathogens. *Nature reviews. Microbiology* **2006,** *4* (2), 91-101.

3. Qualmann, B.; Kessels, M. M., New players in actin polymerization--WH2-domain-containing actin nucleators. *Trends in cell biology* **2009,** *19* (6), 276-85.

4. Stevens, M. P.; Stevens, J. M.; Jeng, R. L.; Taylor, L. A.; Wood, M. W.; Hawes, P.; Monaghan, P.; Welch, M. D.; Galyov, E. E., Identification of a bacterial factor required for actin-based motility of *Burkholderia pseudomallei*. *Molecular microbiology* **2005,** *56* (1), 40-53.

5. Sitthidet, C.; Stevens, J. M.; Chantratita, N.; Currie, B. J.; Peacock, S. J.; Korbsrisate, S.; Stevens, M. P., Prevalence and sequence diversity of a factor required for actin-based motility in natural populations of *Burkholderia* species. *Journal of clinical microbiology* **2008,** *46* (7), 2418-22.

6. Sitthidet, C.; Korbsrisate, S.; Layton, A. N.; Field, T. R.; Stevens, M. P.; Stevens, J. M., Identification of motifs of *Burkholderia pseudomallei* BimA required for intracellular motility, actin binding, and actin polymerization. *Journal of bacteriology* **2011,** *193* (8), 1901-10.

7. Lazar Adler, N. R.; Stevens, M. P.; Dean, R. E.; Saint, R. J.; Pankhania, D.; Prior, J. L.; Atkins, T. P.; Kessler, B.; Nithichanon, A.; Lertmemongkolchai, G.; Galyov, E. E., Systematic Mutagenesis of Genes Encoding Predicted Autotransported Proteins of *Burkholderia pseudomallei* Identifies Factors Mediating Virulence in Mice, Net Intracellular Replication and a Novel Protein Conferring Serum Resistance. *PloS one* **2015,** *10* (4), e0121271.

8. Stevens, J. M.; Ulrich, R. L.; Taylor, L. A.; Wood, M. W.; Deshazer, D.; Stevens, M. P.; Galyov, E. E., Actin-binding proteins from *Burkholderia mallei* and *Burkholderia thailandensis* can functionally compensate for the actin-based motility defect of a *Burkholderia pseudomallei bimA* mutant. *Journal of bacteriology* **2005,** *187* (22), 7857-62.

9. (a) Sitthidet, C.; Stevens, J. M.; Field, T. R.; Layton, A. N.; Korbsrisate, S.; Stevens, M. P., Actin-based motility of *Burkholderia thailandensis* requires a central acidic domain of BimA that recruits and activates the cellular Arp2/3 complex. *Journal of bacteriology* **2010,** *192* (19), 5249-52; (b) Benanti, E. L.; Nguyen, C. M.; Welch, M. D., Virulent *Burkholderia* species mimic host actin polymerases to drive actin-based motility. *Cell* **2015,** *161* (2), 348-60.

10. Lu, Q.; Xu, Y.; Yao, Q.; Niu, M.; Shao, F., A polar-localized iron-binding protein determines the polar targeting of *Burkholderia BimA* autotransporter and actin tail formation. *Cellular microbiology* **2015,** *17* (3), 408-24.

11. (a) Wong, J.; Chen, Y.; Gan, Y. H., Host Cytosolic Glutathione Sensing by a Membrane Histidine Kinase Activates the Type VI Secretion System in an Intracellular Bacterium. *Cell host & microbe* **2015,** *18* (1), 38-48; (b) Schell, M. A.; Ulrich, R. L.; Ribot, W. J.; Brueggemann, E. E.; Hines, H. B.; Chen, D.; Lipscomb, L.; Kim, H. S.; Mrazek, J.; Nierman, W. C.; Deshazer, D., Type VI secretion is a major virulence determinant in *Burkholderia mallei*. *Molecular microbiology* **2007,** *64* (6), 1466-85.

27

12.   Breitbach, K.; Rottner, K.; Klocke, S.; Rohde, M.; Jenzora, A.; Wehland, J.; Steinmetz, I., Actin-based motility of *Burkholderia pseudomallei* involves the Arp 2/3 complex, but not N-WASP and Ena/VASP proteins. *Cellular microbiology* **2003,** *5* (6), 385-93.

13.   (a) David, V.; Gouin, E.; Troys, M. V.; Grogan, A.; Segal, A. W.; Ampe, C.; Cossart, P., Identification of cofilin, coronin, Rac and capZ in actin tails using a *Listeria* affinity approach. *Journal of cell science* **1998,** *111 (Pt 19)*, 2877-84; (b) Van Troys, M.; Lambrechts, A.; David, V.; Demol, H.; Puype, M.; Pizarro-Cerda, J.; Gevaert, K.; Cossart, P.; Vandekerckhove, J., The actin propulsive machinery: the proteome of *Listeria monocytogenes* tails. *Biochemical and biophysical research communications* **2008,** *375* (2), 194-9.

14.   Maegraith, B. G.; Leithead, C. S., Melioidosis: A Case-Report. *Lancet* **1964,** *1* (7338), 862-3.

15.   Choi, K. H.; Kumar, A.; Schweizer, H. P., A 10-min method for preparation of highly electrocompetent *Pseudomonas aeruginosa* cells: application for DNA fragment transfer between chromosomes and plasmid transformation. *Journal of microbiological methods* **2006,** *64* (3), 391-7.

16.   Milton, D. L.; O'Toole, R.; Horstedt, P.; Wolf-Watz, H., Flagellin A is essential for the virulence of *Vibrio anguillarum*. *Journal of bacteriology* **1996,** *178* (5), 1310-9.

17.   Logue, C. A.; Peak, I. R.; Beacham, I. R., Facile construction of unmarked deletion mutants in *Burkholderia pseudomallei* using *sacB* counter-selection in sucrose-resistant and sucrose-sensitive isolates. *Journal of microbiological methods* **2009,** *76* (3), 320-3.

18.   Kersey, P. J.; Duarte, J.; Williams, A.; Karavidopoulou, Y.; Birney, E.; Apweiler, R., The International Protein Index: an integrated database for proteomics experiments. *Proteomics* **2004,** *4* (7), 1985-8.

19.   Taylor, G. K.; Goodlett, D. R., Rules governing protein identification by mass spectrometry. *Rapid communications in mass spectrometry : RCM* **2005,** *19* (23), 3420.

20.   Stevens, M. P.; Friebel, A.; Taylor, L. A.; Wood, M. W.; Brown, P. J.; Hardt, W. D.; Galyov, E. E., A *Burkholderia pseudomallei* type III secreted protein, BopE, facilitates bacterial invasion of epithelial cells and exhibits guanine nucleotide exchange factor activity. *Journal of bacteriology* **2003,** *185* (16), 4992-6.

21.   Cuccui, J.; Milne, T. S.; Harmer, N.; George, A. J.; Harding, S. V.; Dean, R. E.; Scott, A. E.; Sarkar-Tyson, M.; Wren, B. W.; Titball, R. W.; Prior, J. L., Characterization of the *Burkholderia pseudomallei* K96243 capsular polysaccharide I coding region. *Infection and immunity* **2012,** *80* (3), 1209-21.

22.   Schell, M. A.; Zhao, P.; Wells, L., Outer membrane proteome of *Burkholderia pseudomallei* and *Burkholderia mallei* from diverse growth conditions. *Journal of proteome research* **2011,** *10* (5), 2417-24.

23.   Vander Broek, C. W.; Chalmers, K. J.; Stevens, M. P.; Stevens, J. M., Quantitative Proteomic Analysis of *Burkholderia pseudomallei* Bsa Type III Secretion System Effectors Using Hypersecreting Mutants. *Molecular & cellular proteomics : MCP* **2015,** *14* (4), 905-16.

28

24.   Harding, S. V.; Sarkar-Tyson, M.; Smither, S. J.; Atkins, T. P.; Oyston, P. C.; Brown, K. A.; Liu, Y.; Wait, R.; Titball, R. W., The identification of surface proteins of *Burkholderia pseudomallei*. *Vaccine* **2007,** *25* (14), 2664-72.

25.   (a) Su, Y. C.; Wan, K. L.; Mohamed, R.; Nathan, S., A genome level survey of *Burkholderia pseudomallei* immunome expressed during human infection. *Microbes and infection / Institut Pasteur* **2008,** *10* (12-13), 1335-45; (b) Felgner, P. L.; Kayala, M. A.; Vigil, A.; Burk, C.; Nakajima-Sasaki, R.; Pablo, J.; Molina, D. M.; Hirst, S.; Chew, J. S.; Wang, D.; Tan, G.; Duffield, M.; Yang, R.; Neel, J.; Chantratita, N.; Bancroft, G.; Lertmemongkolchai, G.; Davies, D. H.; Baldi, P.; Peacock, S.; Titball, R. W., A *Burkholderia pseudomallei* protein microarray reveals serodiagnostic and cross-reactive antigens. *Proceedings of the National Academy of Sciences of the United States of America* **2009,** *106* (32), 13499-504.

26.   (a) Nieves, W.; Asakrah, S.; Qazi, O.; Brown, K. A.; Kurtz, J.; Aucoin, D. P.; McLachlan, J. B.; Roy, C. J.; Morici, L. A., A naturally derived outer-membrane vesicle vaccine protects against lethal pulmonary *Burkholderia pseudomallei* infection. *Vaccine* **2011,** *29* (46), 8381-9; (b) Nieves, W.; Petersen, H.; Judy, B. M.; Blumentritt, C. A.; Russell-Lodrigue, K.; Roy, C. J.; Torres, A. G.; Morici, L. A., A *Burkholderia pseudomallei* outer membrane vesicle vaccine provides protection against lethal sepsis. *Clinical and vaccine immunology : CVI* **2014,** *21* (5), 747-54.

27.   Kim, H.; White, C. D.; Sacks, D. B., IQGAP1 in microbial pathogenesis: Targeting the actin cytoskeleton. *FEBS letters* **2011,** *585* (5), 723-9.

28.   Haglund, C. M.; Choe, J. E.; Skau, C. T.; Kovar, D. R.; Welch, M. D., *Rickettsia* Sca2 is a bacterial formin-like mediator of actin-based motility. *Nature cell biology* **2010,** *12* (11), 1057-63.

29.   (a) Welch, M. D.; Iwamatsu, A.; Mitchison, T. J., Actin polymerization is induced by Arp2/3 protein complex at the surface of *Listeria monocytogenes*. *Nature* **1997,** *385* (6613), 265-9; (b) Welch, M. D.; Rosenblatt, J.; Skoble, J.; Portnoy, D. A.; Mitchison, T. J., Interaction of human Arp2/3 complex and the *Listeria monocytogenes* ActA protein in actin filament nucleation. *Science* **1998,** *281* (5373), 105-8.

30.   Loisel, T. P.; Boujemaa, R.; Pantaloni, D.; Carlier, M. F., Reconstitution of actin-based motility of *Listeria* and *Shigella* using pure proteins. *Nature* **1999,** *401* (6753), 613-6.

31.   Van Kirk, L. S.; Hayes, S. F.; Heinzen, R. A., Ultrastructure of *Rickettsia rickettsii* actin tails and localization of cytoskeletal proteins. *Infection and immunity* **2000,** *68* (8), 4706-13.

32.   (a) Mateer, S. C.; Morris, L. E.; Cromer, D. A.; Bensenor, L. B.; Bloom, G. S., Actin filament binding by a monomeric IQGAP1 fragment with a single calponin homology domain. *Cell motility and the cytoskeleton* **2004,** *58* (4), 231-41; (b) Erickson, J. W.; Cerione, R. A.; Hart, M. J., Identification of an actin cytoskeletal complex that includes IQGAP and the Cdc42 GTPase. *The Journal of biological chemistry* **1997,** *272* (39), 24443-7.

Synopsis description and image

The BimA protein of the melioidosis pathogen *Burkholderia pseudomallei* recruits and polymerises cellular actin to promote motility within the host cell cytosol ls. The mechanism by which BimA subverts the cellular cytoskeletal machinery is understudied. We have used an affinity approach coupled with Mass Spectrometry to identify cellular proteins involved in tail formation, demonstrating that IQGAP1 participates in determining both the length and actin density of these structures.

For TOC only

30

1
2
3
4
5
6
7 **Figure 1**
8
9
10
11
12
13
14
15
16
17
18
19
20
21
22
23
24
25
26
27
28
29
30
31
32
33
34
35
36
37
38
39
40
41
42
43
44
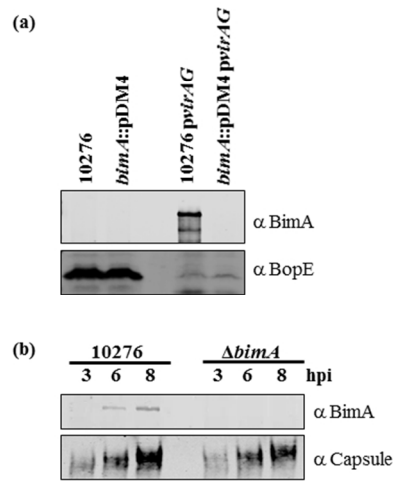45
46
47
48
49
50
51
52
53
54
55
56
57
58
59
60
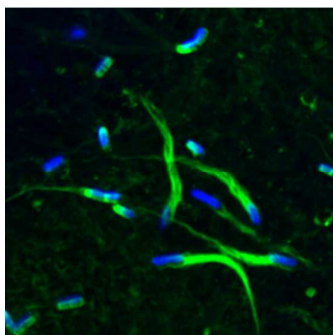
Figure 1
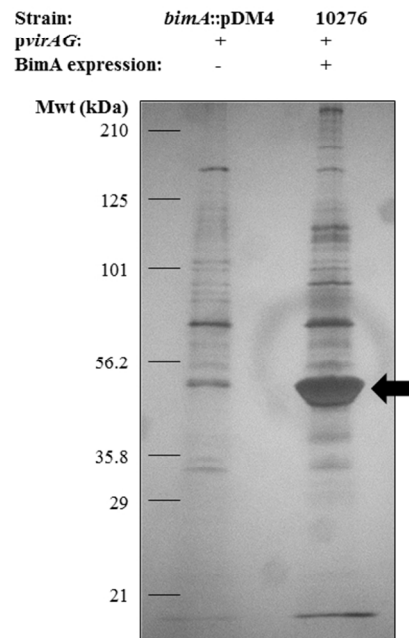
254x190mm (96 x 96 DPI)

Figure 2

Figure 2

254x190mm (96 x 96 DPI)

1
2
3
4
5
6
7
8
9
10
11
12
13
14
15
16
17
18
19
20
21
22
23
24
25
26
27
28
29
30
31
32
33
34
35
36
37
38
39
40
41
42
43
44
45
46
47
48
49
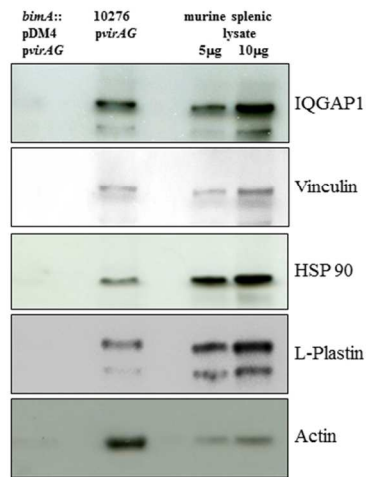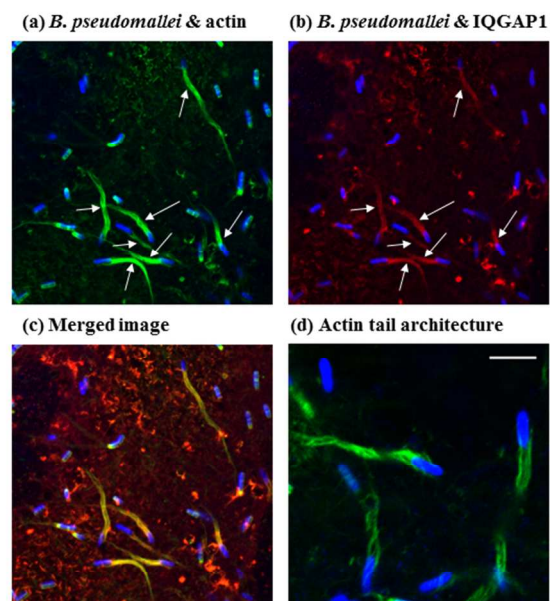50
51
52
53
54
55
56
57
58
59
60

Figure 3

Figure 3

254x190mm (96 x 96 DPI)

Figure 4

(a) *B. pseudomallei* & actin
(b) *B. pseudomallei* & IQGAP1
(c) Merged image
(d) Actin tail architecture

Figure 4

254x190mm (96 x 96 DPI)

1
2
3
4
5
6
7
8
9
10
11
12
13
14
15
16
17
18
19
20
21
22
23
24
25
26
27
28
29
30
31
32
33
34
35
36
37
38
39
40
41
42
43
44
45
46
47
48
49
50
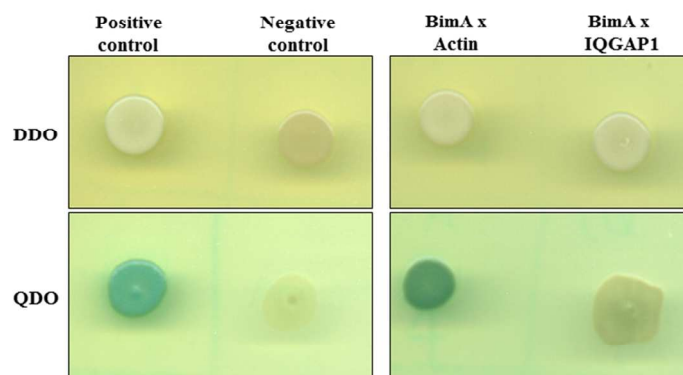51
52
53
54
55
56
57
58
59
60

Figure 5

Figure 5

254x190mm (96 x 96 DPI)

1
2
3
4
5
6
7
8
9
10
11
12
13
14
15
16
17
18
19
20
21
22
23
24
25
26
27
28
29
30
31
32
33
34
35
36
37
38
39
40
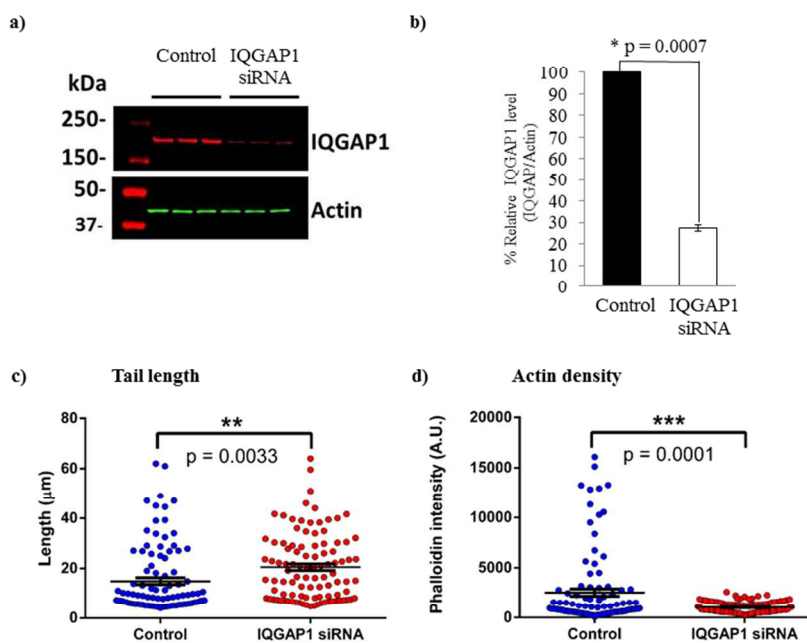41
42
43
44
45
46
47
48
49
50
51
52
53
54
55
56
57
58
59
60

Figure 6

Figure 6

254x190mm (96 x 96 DPI)